Ca^{2+}-Activated K^+ Channel–3.1 Blocker TRAM-34 Attenuates Airway Remodeling and Eosinophilia in a Murine Asthma Model

Pierre-Olivier Girodet[1,2,3], Annaig Ozier[1,2,3], Gabrielle Carvalho[1,2], Olga Ilina[1,2], Olga Ousova[1,2], Alain-Pierre Gadeau[1,2], Hugues Begueret[3], Heike Wulff[4], Roger Marthan[1,2,3], Peter Bradding[5], and Patrick Berger[1,2,3]

[1]Centre de Recherche Cardio-Thoracique de Bordeaux, U1045, U1034, Département de Pharmacologie, CIC 0005, University of Bordeaux, Bordeaux, France; [2]Centre de Recherche Cardio-Thoracique de Bordeaux, INSERM, U1045, U1034, CIC 0005, Université Bordeaux Segalen, Bordeaux, France; [3]Service d'Exploration Fonctionnelle Respiratoire, and Service d'Anatomopathologie, CIC 0005, CHU de Bordeaux, Pessac, France; [4]Department of Pharmacology, University of California at Davis, Davis, California; and [5]Department of Infection, Immunity, and Inflammation, Institute for Lung Health, University of Leicester Medical School, Leicester, United Kingdom

Key features of asthma include bronchial hyperresponsiveness (BHR), eosinophilic airway inflammation, and bronchial remodeling, characterized by subepithelial collagen deposition, airway fibrosis, and increased bronchial smooth muscle (BSM) mass. The calcium-activated K^+ channel $K_{Ca}3.1$ is expressed by many cells implicated in the pathogenesis of asthma, and is involved in both inflammatory and remodeling responses in a number of tissues. The specific $K_{Ca}3.1$ blocker 5-[(2-chlorophenyl)(diphenyl)methyl]-1*H*-pyrazole (TRAM-34) attenuates BSM cell proliferation, and both mast cell and fibrocyte recruitment *in vitro*. We aimed to examine the effects of $K_{Ca}3.1$ blockade on BSM remodeling, airway inflammation, and BHR in a murine model of chronic asthma. BALB/c mice were sensitized with intraperitoneal ovalbumin (OVA) on Days 0 and 14, and then challenged with intranasal OVA during Days 14–75. OVA-sensitized/challenged mice received TRAM-34 (120 mg/kg/day, subcutaneous) from Days −7 to 75 (combined treatment), Days −7 to 20 (preventive treatment), or Days 21 to 75 (curative treatment). Untreated mice received daily injections of vehicle ($n = 8$ per group). Bronchial remodeling was assessed by histological and immunohistochemical analyses. Inflammation was evaluated using bronchoalveolar lavage and flow cytometry. We also determined BHR in both conscious and anesthetized mice via plethysmography. We demonstrated that curative treatment with TRAM-34 abolishes BSM remodeling and subbasement collagen deposition, and attenuates airway eosinophilia. Although curative treatment alone did not significantly reduce BHR, the combined treatment attenuated nonspecific BHR to methacholine. This study indicates that $K_{Ca}3.1$ blockade could provide a new therapeutic strategy in asthma.

CLINICAL RELEVANCE

The calcium-activated K^+ channel $K_{Ca}3.1$ is implicated in asthma pathogenesis. However, the effects of $K_{Ca}3.1$ blockade on both inflammatory and remodeling processes has not been explored so far in a murine model of chronic asthma. This study reports that curative treatment with the $K_{Ca}3.1$ blocker 5-[(2-chlorophenyl)(diphenyl)methyl]-1*H*-pyrazole (TRAM-34) abolishes bronchial smooth muscle remodeling and subbasement collagen deposition, and attenuates airway eosinophilia in a murine model of chronic asthma. Moreover, the combination of both preventive and curative treatment reduced nonspecific bronchial hyperresponsiveness to methacholine. Blocking $K_{Ca}3.1$ has great potential in the treatment of chronic asthma by preventing the increased mass of bronchial smooth muscle associated with airway remodeling.

Keywords: asthma; $K_{Ca}3.1$; ion channel; remodeling; smooth muscle

Asthma is a chronic airway disease characterized by bronchial hyperresponsiveness (BHR), persistent airway inflammation, and remodeling (1, 2). Bronchial remodeling comprises abnormal airway epithelium, subepithelial collagen deposition, extracellular matrix deposition, neoangiogenesis, mucus gland hypertrophy, and an increased bronchial smooth muscle (BSM) mass (3). It likely contributes to the development of fixed airflow obstruction, which occurs in many patients with longstanding disease (4, 5), and current treatments such as inhaled and oral corticosteroids appear ineffective at preventing or reversing this feature of asthma (6). At a cellular level, BSM cells can orchestrate chronic inflammation through the production of chemotactic factors, and may themselves contribute to the development of remodeling through the promotion of inflammation and the secretion of profibrotic and mitogenic growth factors (7). For example, BSM-derived cytokines/chemokines induce the recruitment of T lymphocytes and mast cells that infiltrate and adhere to the BSM (8–14), which may in turn promote BSM dysfunction (15). More recently, an increased proliferation of asthmatic BSM cells has been demonstrated *ex vivo* (16). This increased proliferative potential persists *in vitro* (17), and is triggered, at least in part, by altered calcium homeostasis (18, 19), leading to a high level of mitochondrial biogenesis (18). Because corticosteroids remain totally ineffective at decreasing BSM proliferation and mass (6), targeting BSM cells represents an interesting strategy to prevent and treat bronchial remodeling in asthma.

K^+ channels control plasma membrane potential in several cell types, including BSM cells, (20, 21) and thus modulate Ca^{2+}

(*Received in original form March 14, 2012 and in final form November 16, 2012*)

O.I. was funded by the Bourse Charcot from the Ministère des Affaires Étrangères et Européennes of France. H.W. was funded by the American Recovery and Reinvestment Act Stimulus Fund through National Institutes of Health grant R01GM076063-04S1.

Author Contributions: P.-O.G., P. Bradding, and P. Berger were responsible for the conception and design of this study. P.-O.G., A.O., O.I., O.O., A.-P.G., H.B., H.W., R.M., P. Bradding, and P. Berger were responsible for analysis and interpretation. P.-O.G., H.W., R.M., P. Bradding, and P. Berger were responsible for drafting the manuscript in terms of important intellectual content. P.-O.G., H.W., R.M., P. Bradding, and P. Berger were responsible for revising the manuscript in terms of important intellectual content. P.-O.G., A.O., O.I., O.O., H.W., R.M., P. Bradding, and P. Berger were responsible for final approval of the manuscript.

Correspondence and requests for reprints should be addressed to Patrick Berger, M.D., Ph.D., Centre de Recherche Cardio-Thoracique de Bordeaux, INSERM, U1045, Université Bordeaux Segalen, 146 Rue Léo Saignat, 33076 Bordeaux Cedex, France. E-mail: patrick.berger@u-bordeaux2.fr

This article has an online supplement, which is accessible from this issue's table of contents at www.atsjournals.org

Am J Respir Cell Mol Biol Vol 48, Iss. 2, pp 212–219, Feb 2013
Copyright © 2013 by the American Thoracic Society
Originally Published in Press as DOI: 10.1165/rcmb.2012-0103OC on November 29, 2012
Internet address: www.atsjournals.org

signaling. Among the three major families of human Ca^{2+}-activated K^+ channels (K_{Ca}), the intermediate-conductance $K_{Ca}3.1$ is of particular interest in bronchial remodeling (22) because it is expressed in epithelial cells (23, 24), fibroblasts (25), human lung mast cells (26), asthmatic BSM cells (27), and fibrocytes (28). Moreover, $K_{Ca}3.1$ plays a role in a variety of cell functions relevant to asthma (29), including proliferation, cell activation, and chemotaxis (22). For example, functional $K_{Ca}3.1$ channels regulate BSM proliferation (27), and the specific $K_{Ca}3.1$ blockers TRAM-34 and ICA-17043 (senecapoc; Icagen, Durham, NC) markedly attenuate human lung mast cell (30) and human fibrocyte migration (28) in response to numerous stimuli, including cytokines/chemokines present in BSM supernatants (28). However, the potential effects of $K_{Ca}3.1$ blockade on BSM remodeling, as well as BHR and airway inflammation, remain to be confirmed *in vivo*. Thus, this study sought to examine the effects of the $K_{Ca}3.1$ blocker 5-[(2-chlorophenyl)(diphenyl)methyl]-1*H*-pyrazole (TRAM-34) on key features of asthma pathophysiology in a murine model of chronic asthma.

MATERIALS AND METHODS

Chronic Model of Murine Asthma

Female BALB/c mice (Elevage Janvier, Le Genest Saint Isle, France) were sensitized with an intraperitoneal injection of 100 μg ovalbumin (OVA; Sigma-Aldrich, Saint-Quentin-Fallavier, France) in NaCl 0.9% (B. Braun Medical, Boulogne Billancourt, France), without aluminum hydroxide, on Days 0 and 14 (31). Anesthetized mice received intranasal OVA periodically on Days 14 to 75 (31, 32). The control group received NaCl 0.9% intraperitoneally on Days 0 and 14, and intranasally on Days 14 to 75. The Institutional Animal Ethics Committee (Bordeaux University, Bordeaux, France) approved all animal use procedures.

Study Design

TRAM-34 (33) was dissolved in neutral oil (Miglyol-812; Caesar and Loretz GmbH, Hilden, Germany) and administered once daily subcutaneously at 120 mg/kg/day. Four groups of OVA-sensitized and challenged mice (OVA mice) received daily injections of either (*1*) Miglyol-812 from Days −7 to 75 (untreated group); (*2*) TRAM-34 from Days −7 to 75 (i.e., before intraperitoneal sensitization and during nasal challenge; the combined treatment group); (*3*) TRAM-34 before and during intraperitoneal sensitization (Days −7 to 20) and Miglyol-812 during nasal challenge (Days 21–75; the preventive treatment group); or (*4*) Miglyol-812 before and during intraperitoneal sensitization (Days −7 to 20) and TRAM-34 during nasal challenge (Days 21–75; the curative treatment group).

Determination of Bronchial Hyperresponsiveness

Nonspecific BHR to methacholine (Sigma-Aldrich) was measured in both unrestrained, conscious mice by single-chamber plethysmography on Days 0, 20, and 76, and in anesthetized mice by invasive plethysmography (Emka Technologies, Paris, France) on Day 80. Enhanced pause (Penh) and lung resistance (Rs) were expressed as a ratio of values measured in response to methacholine to those with normal saline. Specific BHR to OVA was measured 4 hours after intranasal OVA challenge on Days 28 and 74.

Tissue Sampling

Peripheral blood was recovered on Day 78 by retro-orbital bleeding. Bronchoalveolar lavage (BAL), bone marrow, lung digest cells, and liver tissue were collected on Day 80 (*see* the online supplement for details).

ELISA

BAL fluid concentrations of IL-4, IL-13, and activated TGF-β1 were determined by ELISA (R&D Systems, Lille, France).

Histological and Immunohistochemical Analyses

Paraffin-embedded sections were stained with hematoxylin-eosin-safran or Masson trichrome. Immunohistochemistry was processed using an anti-mouse α–smooth muscle actin (Sigma-Aldrich) and anti-mouse CD31 (BMA Biomedicals, Augst, Switzerland). Several quantitative parameters were assessed using Quancoul (Quant'Image, Bordeaux, France) software: wall area, BSM area, subbasement membrane thickness (BMT), basement membrane length (BML), peribronchial fibrosis (PBF), and the number of nucleated cells within the peribronchial space (see the online supplement for details).

Flow Cytometry

Cells were stained using antibodies directed against CD3-ε, CD4, CD8a, CD90.2, CD117 (*c-kit*), CD49b/Pan-NK cells (all from BD Biosciences–Pharmingen, Le Pont de Claix, France), CD25 (eBioscience, Paris, France), and Foxp3 (eBioscience) (*see* the online supplement for details).

Statistical Analysis

Values are expressed as the mean ± SEM. The data were analyzed using NCSS 2001 software (NCSS Statistical Software, Kaysville, UT) with the Mann-Whitney test. Multiple comparisons were performed by means of Kruskal-Wallis ANOVA, with the use of multiple-comparisons z-tests. $P < 0.05$ was considered statistically significant.

RESULTS

Characterization of the Chronic Model of Murine Asthma

Nonspecific BHR in response to nebulized methacholine was assessed using both noninvasive and invasive plethysmography (Figure 1). We first checked the absence of spontaneous BHR in mice on Day 0 (Figure 1A). Six days after the first intranasal challenge (Day 20), the Penh ratio was already significantly increased in OVA-challenged mice, compared with that of saline-challenged mice ($P < 0.001$; Figure 1B). OVA-challenged animals maintained BHR to methacholine on Day 76, 24 hours after the last intranasal challenge ($P < 0.001$ versus the control group; Figure 1C). Similar results were obtained using invasive plethysmography on Day 80 ($P < 0.01$, OVA versus saline; Figure 1D).

We also assessed airway inflammation, using both BAL fluid and cells obtained from digested lungs. To determine the onset of inflammatory leukocyte influx into the lung, BAL was performed in two sets of experiments on Day 20 (*see* Figures E1A, E1C, and E1E in the online supplement) or on Day 80 (see Figures E1B, E1D, and E1F). The total number of cells was unchanged in the BAL fluid from OVA-challenged mice on Day 20 (Figure E1A), but was significantly increased on Day 80, with a 3.5-fold higher value compared with control mice ($P < 0.01$; see Figure E1B). This finding on Day 80 was confirmed with a significant increase in the total number of lung cells (Figure E2A). However, on both Day 20 and Day 80, percentages of both eosinophils and lymphocytes were increased in OVA-challenged mice, compared with saline-exposed animals (Figures E1C–E1F). Moreover, the number of $CD4^+$ T lymphocytes was increased within the lungs of OVA-challenged mice (Figure E2B), resulting in a higher CD4/CD8 ratio on Day 80 compared with that of control mice (Figure E2C).

We then assessed bronchial remodeling, using morphometric analyses of bronchial slices obtained on Day 20 or on Day 80. As expected, no features of bronchial remodeling on Day 20 were evident (data not shown). However, OVA-challenged mice exhibited structural features associated with airway remodeling on Day 80 (Figure 2A) compared with control mice (Figure 2B), including a significant increase in subbasement membrane thickness (Figure 2C), normalized BSM area (Figure 2D), and peribronchial fibrosis (Figure 2E).

Finally, endothelial cell staining with anti-CD31 antibody did not indicate any neoangiogenesis in OVA-challenged mice, compared with control mice (Figure E3).

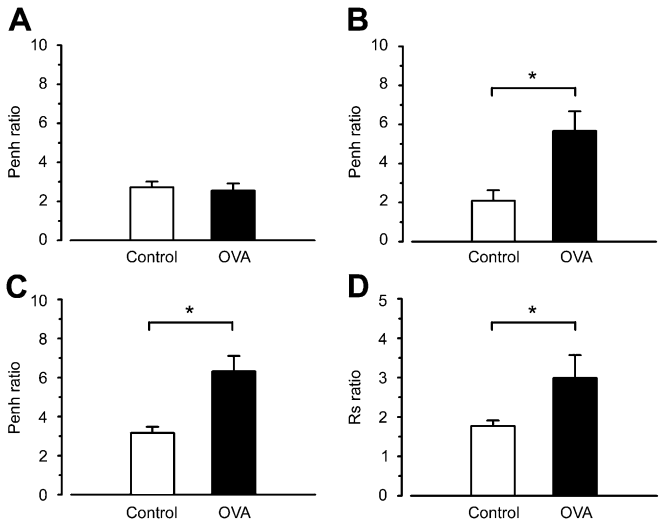

Figure 1. Chronic airway exposure of mice to ovalbumin (OVA) increased the bronchial contractile response to methacholine. BALB/c mice received either OVA (*solid bars*) or normal saline (*open bars*). Bronchial hyperresponsiveness (BHR) to methacholine was determined in both unrestrained conscious mice by single-chamber plethysmography (*A*–*C*) and anesthetized mice by invasive plethysmography (*D*). Both the enhanced pause parameter (Penh) and lung resistance (Rs) were measured and averaged for 3 minutes, 30 seconds after nebulized methacholine (8 mg/ml). Penh measurements were performed on Days 0 (*A*, $n = 29$), 20 (*B*, $n = 14$), and 76 (*C*, $n = 29$), and expressed as a ratio of Penh measured in response to methacholine to that with normal saline. Lung Rs measurements were performed on Day 80 (*D*, $n = 9$), and expressed as a ratio of Rs measured in response to methacholine to that with normal saline. Data represent the mean ± SEM. *$P < 0.05$, according to the Mann-Whitney test.

$K_{Ca}3.1$ Blockade Attenuated Nonspecific BHR

We first tested whether TRAM-34 exerts any effect on nonspecific and specific BHR in this model of chronic allergic asthma. Pretreatment with either Miglyol-812 (vehicle) or TRAM-34 from Day −7 to Day 0 did not affect lung function assessed before the first intraperitoneal injection of OVA (Figure 3A). The combined treatment with TRAM-34, administered during both the sensitization and the challenge phases, induced a significant inhibition of BHR to methacholine on Day 76 (Figure 3B). Conversely, preventive or curative treatment with TRAM-34 did not alter nonspecific BHR. Moreover, specific BHR to OVA was not altered by TRAM-34, whatever the administration protocol (data not shown).

$K_{Ca}3.1$ Blockade Attenuates Eosinophilic Inflammation and Th2 Cytokine Production

We next examined the role of $K_{Ca}3.1$ blockade on the recruitment of inflammatory cells within the lung. The combined treatment with TRAM-34 during both the sensitization and the challenge phases significantly decreased the total cell count and the percentage of eosinophils in the BAL fluid collected on Day 80 (Figures 4A and 4B), although both remained higher than in control mice (Figures E1B and E1D). Moreover, percentages of lymphocytes (Figure 4C), neutrophils, and macrophages (data not shown) were not significantly altered in the BAL fluid. Furthermore, the combined treatment with TRAM-34 did not alter the total cell number (Figure 4D), the absolute numbers of $CD4^+$ T lymphocytes (Figure 4E), natural killer T (NKT) cells (data not shown), and regulatory T cells (Tregs) (data not shown), or the CD4/CD8 ratio (Figure 4F) within the digested lung.

When TRAM-34 was administered preventively during the sensitization phase only, no significant changes were evident in any inflammatory parameter assessed in the BAL fluid or in the digested lung tissue (Figures 4A–4F). When TRAM-34 was administered curatively during the challenge phase only, the total cell number and the percentage of lymphocytes were unchanged in the BAL fluid (Figures 4A and 4C). However, we again observed a significant decrease in the percentage of eosinophils (Figure 4B). These treatments did not alter total cell or T-cell parameters in digested lung tissue (Figures 4D–4F).

In addition, TRAM-34 did not change any inflammatory parameters assessed on Day 80 by lung histology (i.e., bronchial wall surface normalized to BML, peribronchovascular space area, and number of nucleated cells within the peribronchial space; data not shown). Likewise, blood T lymphocyte, bone marrow progenitor ($CD90^+CD117^+$), and lung mast cell expression remained unchanged in all TRAM-34 treatment groups (data not shown).

Significant concentrations of IL-4, IL-13, and activated TGF-β1 were found in the BAL fluid of OVA-sensitized/challenged mice compared with the saline control group (54.4 ± 8.9 pg/ml

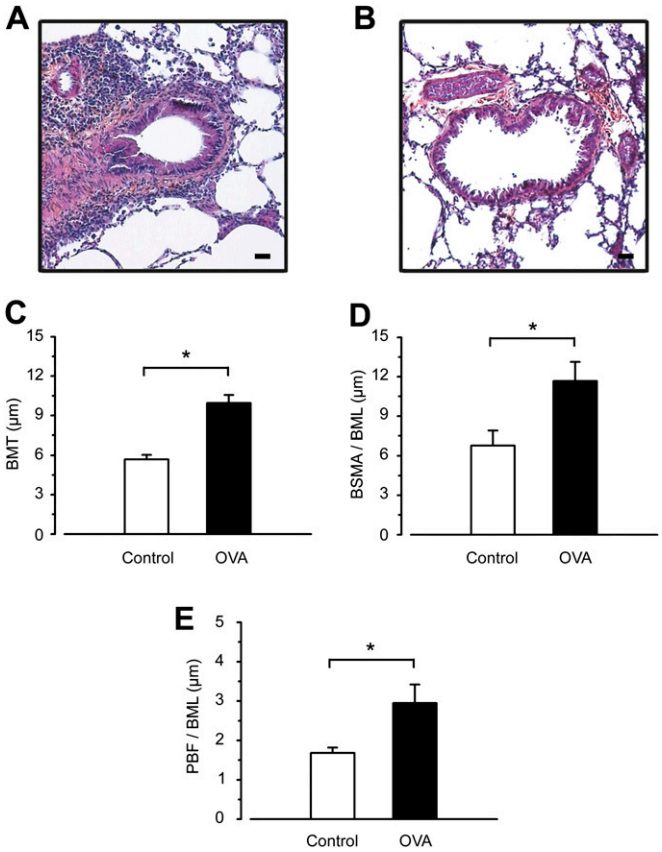

Figure 2. Chronic airway exposure of mice to OVA reproduced bronchial remodeling. Representative sections of bronchial tissue were obtained from control mice (*A*) and OVA-sensitized/challenged mice (*B*). Sections were stained with hematoxylin-eosin-safran (HES). *Scale bars* represent 50 μm (×100 magnification). Quantitative parameters were assessed on Day 80, using Quancoul software (Quant'Image, Bordeaux, France) on lung slices stained with HES (*C*), α-smooth muscle actin (*D*), or Masson trichrome (*E*) at ×100 magnification. BALB/c mice received either OVA (*solid bars*, $n = 15$) or normal saline (*open bars*, $n = 15$). The subbasement membrane thickness (BMT), the bronchial smooth muscle area/basement membrane length ratio (BSMA/BML), and the peribronchial fibrosis/basement membrane length ratio (PBF/BML) were significantly higher in asthmatic mice than in control mice. Data represent the mean ± SEM. *$P < 0.05$, according to the Mann-Whitney test.

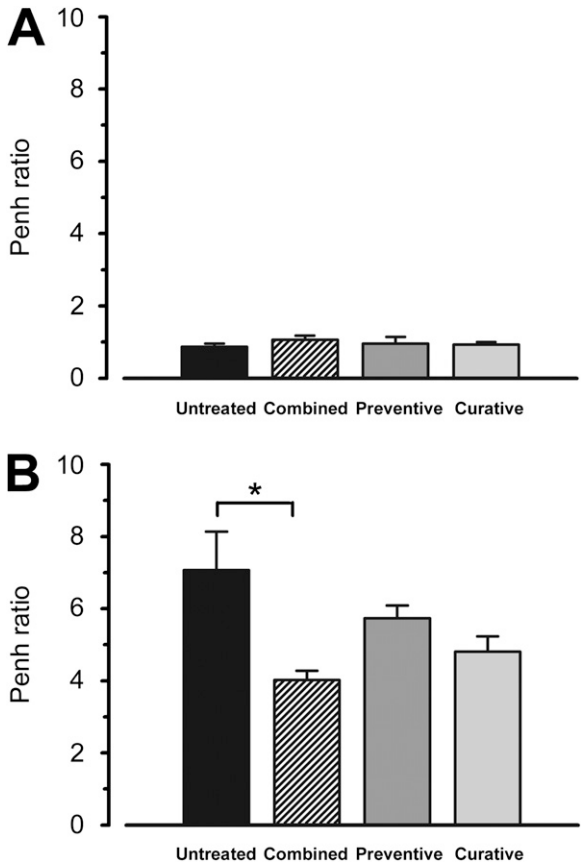

Figure 3. Effects of 5-[(2-chlorophenyl)(diphenyl)methyl]-1*H*-pyrazole (TRAM-34) on bronchial hyperresponsiveness to methacholine. OVA-sensitized/challenged mice received daily subcutaneous injections of TRAM-34 or its vehicle Miglyol-812 from Day −7 to Day 75. Penh measurements were performed on Days 0 (*A*) and 76 (*B*), and expressed as a ratio of Penh measured in response to methacholine to that with normal saline. OVA mice received Miglyol-812 from Day −7 to Day 75 (untreated group, *solid bars*), or TRAM-34 from Day −7 to Day 75 (combined treatment, *hatched bars*), TRAM-34 from Day −7 to Day 20, and Miglyol-812 from Days 21–75 (preventive treatment, *dark gray bars*), or Miglyol-812 from Day −7 to Day 20 and TRAM-34 from Days 21–75 (curative treatment, *light gray bars*) ($n = 8$ per group). Data represent the mean ± the SEM. $^*P < 0.05$ between populations within an experimental condition, using the Kruskal-Wallis test along with the multiple-comparisons z-test.

versus 20.7 ± 8.7 pg/ml, 34.5 ± 9.9 pg/ml versus 0 ± 0 pg/ml, and 410.4 ± 88.1 pg/ml versus 0 ± 0 pg/ml, respectively; $P < 0.05$). Significant reductions of 89.0% and 58.0% in BAL fluid concentrations of IL-4 and IL-13, respectively, were seen in OVA mice treated with TRAM-34 from Day −7 to Day 75, compared with untreated OVA mice (Figures 5A and 5B). Moreover, when TRAM-34 was administered curatively during the challenge phase only, the concentration of IL-4 was also significantly reduced. Conversely, TRAM-34 did not induce a significant decrease in BAL fluid TGF-β1 concentrations (Figure 5C).

$K_{Ca}3.1$ Channel Blockade Abolishes Bronchial Remodeling

We then determined the effects of the pharmacological inhibition of $K_{Ca}3.1$ channels on bronchial remodeling. Compared with control mice (Figures 6A and 6B), untreated OVA-sensitized/challenged mice (Figures 6C and 6D) exhibited characteristics of bronchial remodeling, which were abolished in mice treated with TRAM-34 from Day −7 to Day 75 (Figures 6E and 6F). Indeed, the combined treatment with TRAM-34, administered during both the sensitization and challenge phases, significantly reduced subbasement membrane thickness (Figure 7A) and normalized both BSM area (Figure 7B) and bronchial collagen deposition/fibrosis (Figure 7C) in "asthmatic" mice on Day 80, compared with untreated animals. All these parameters reached the levels assessed in control mice (Figure 2).

Preventive treatment with TRAM-34 moderately reduced subbasement membrane thickness (Figure 7A), but did not change normalized BSM area (Figure 7B) or bronchial collagen deposition/fibrosis (Figure 7C). Interestingly, curative treatment with TRAM-34, administered during the challenge phase only, significantly reduced both subbasement membrane thickness (Figure 7A) and normalized BSM area (Figure 7B) to the levels of those assessed in control mice (Figure 2).

Safety of the $K_{Ca}3.1$ Blockade Approach

As previously reported (34), the histology of liver sections revealed no damage induced by the chronic administration of TRAM-34 or its vehicle (Figure E4).

DISCUSSION

In this study, we demonstrate for the first time that curative treatment with the specific $K_{Ca}3.1$ blocker TRAM-34 abolishes BSM remodeling and subbasement collagen deposition, and attenuates airway eosinophilia in a murine model of chronic asthma. Curative treatment alone did not significantly reduce BHR, but the combination of both preventive and curative treatment attenuated nonspecific BHR to methacholine.

We purposefully chose an animal model able to reflect human asthma as accurately as possible. Indeed, we found that OVA-exposed mice expressed the three main characteristics of human asthma, namely, BHR, eosinophilic airway inflammation, and airway remodeling, characterized by subepithelial collagen deposition, airway fibrosis, and increased BSM mass. The use of Penh to assess BHR in mice is controversial, and may vary according to respiratory rate and experimental conditions (35). For instance, Penh is not accurate in C57BL6 mice (36). However, in our study, the Penh ratio was correlated with lung resistance as assessed by invasive plethysmography, which is in agreement with earlier studies performed in BALB/c mice (36). Moreover, invasive plethysmography cannot be performed longitudinally. In our study, we assessed BHR at various time points (i.e., on Days 0, 20, 28, 74, and 76). The close correlation between Penh measurements and invasive plethysmography at the end of the study, and the high reproducibility of Penh in control animals, indicate that this is a valid method to assess BHR in our model. One of the main drawbacks of many animal models of asthma remains the lack of BSM remodeling (37). We adapted the model described by Henderson and colleagues, which used aluminum hydroxide and induced BSM remodeling (32). In this study, we were able to induce BSM remodeling in the absence of any adjuvant, as previously reported (31). Indeed, murine models, performed in the presence of aluminum hydroxide, do not require mast cells (38), whereas in human asthma, the role of this cell type is well known (8).

To date, very few studies have been able to demonstrate a significant effect of any pharmacological compounds on BSM mass in sensitized mice. For instance, montelukast (32) or combined corticosteroid/long-acting bronchodilator treatment (39) have been shown to significantly decrease BSM size only in the context of allergen avoidance (39). The effects of TRAM-34 during the postsensitization phase were striking, with BSM mass no different from that in unchallenged control animals. These *in vivo*

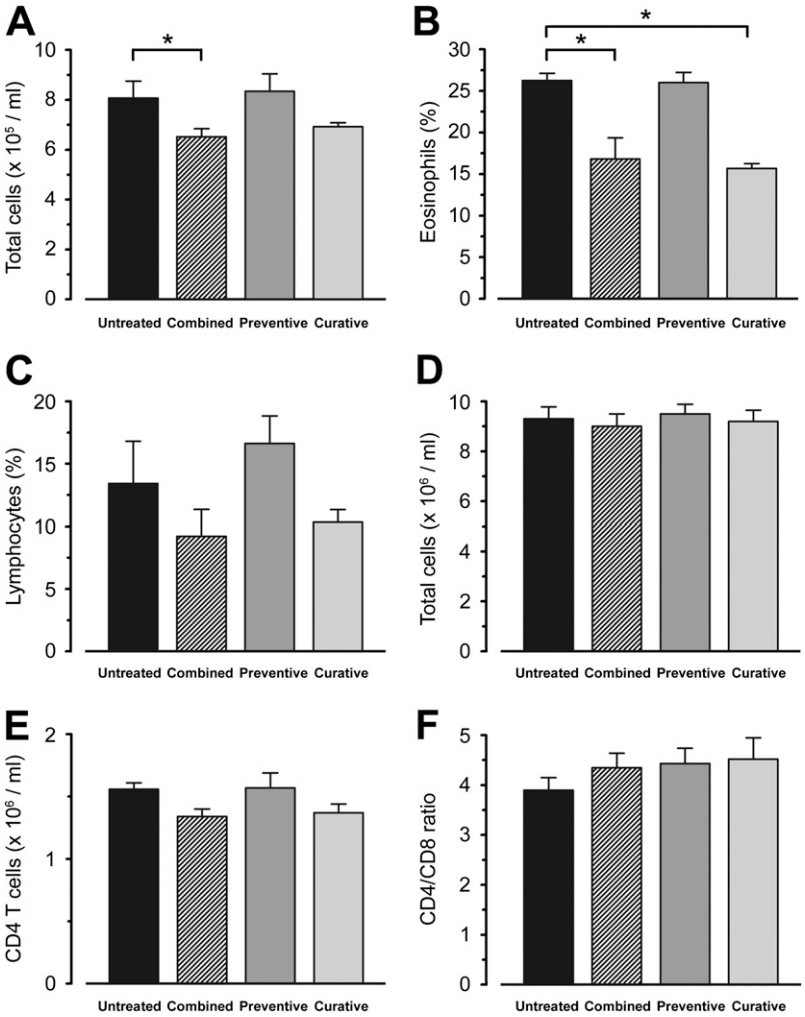

Figure 4. Effects of TRAM-34 on lung inflammation. OVA-sensitized/challenged mice received daily subcutaneous injections of TRAM-34 or its vehicle Miglyol-812 from Day −7 to Day 75. Bronchoalveolar lavage (BAL) fluid was obtained on Day 80 (*A–C*). The total number of lung cells (*D*), the absolute number of CD4 T cells (*E*), and the CD4/CD8 ratio (*F*) were assessed on Day 80, using flow cytometry on cells obtained from digested lungs. OVA mice received Miglyol-812 from Day −7 to Day 75 (untreated group, *solid bars*), or TRAM-34 from Day −7 to Day 75 (combined treatment, *hatched bars*), or TRAM-34 from Day −7 to Day 20 and Miglyol-812 from Days 21–75 (preventive treatment, *dark gray bars*), or Miglyol-812 from Day −7 to Day 20 and TRAM-34 from Days 21–75 (curative treatment, *light gray bars*) ($n = 8$ per group). Data represent the mean ± SEM. $^*P < 0.05$ between populations within an experimental condition, using the Kruskal-Wallis test along with the multiple-comparisons *z*-test.

effects of TRAM-34 on the BSM are in keeping with those previously reported for human BSM cell proliferation *in vitro* (27). Therefore, TRAM-34 was likely to inhibit BSM cell proliferation directly, although inhibition of fibrocyte recruitment (28) or an indirect effect through the attenuation of eosinophilic inflammation might also play a role.

Treatment with TRAM-34 throughout the experimental protocol reduced nonspecific BHR to methacholine. We may have been underpowered to identify a significant difference with curative treatment, but interestingly, a discrepancy was evident between the effect of curative treatment on BHR and BSM mass. This suggests that an element of BHR occurs through increased contractility rather than increased BSM mass *per se*, which is in keeping with several human studies (40, 41).

In human asthma, collagen deposition in the subbasement membrane is associated with airway eosinophilia, and is not present in noneosinophilic disease (42). It is also present in nonasthmatic eosinophilic bronchitis (8). Subbasement membrane collagen deposition appears to be a consequence of eosinophilic inflammation, because it is attenuated in human asthma by anti–IL-5 therapy, which specifically targets eosinophilic inflammation (43). Our observations of parallel reductions in BAL eosinophilia and subbasement membrane collagen deposition with both combined and curative treatments with TRAM-34 are in keeping with these previous observations. However, TRAM-34 may also inhibit airway myofibroblast function, as previously described in renal fibrosis (44).

In vivo, TRAM-34 was administered once daily subcutaneously at a dose of 120 mg/kg/day. For this purpose, we dissolved TRAM-34 in neutral oil. Such dosing was previously well tolerated in mice when continued daily for 3 months in a study evaluating the preventive effects of $K_{Ca}3.1$ blockade on the development of atherosclerosis in $ApoE^{-/-}$ mice (34). Although bioavailability out of the subcutaneous space is low, the repeated subcutaneous administration of the lipophilic TRAM-34 results in steady-state total plasma concentrations of around 800–900 nM (34). Considering TRAM-34's plasma protein binding of 98% (45), these total plasma concentrations render free plasma concentrations of approximately 20 nM, which equal TRAM-34's half-maximal inhibitory concentration for the $K_{Ca}3.1$ channel (33). Because TRAM-34 has always been reported to affect BSM cell and fibroblast function at lower concentrations than T-cell proliferation and cytokine secretion, these relatively low free plasma concentrations might explain why we are predominantly observing effects on BSM mass rather than on immune cell infiltration.

Taken together, our results clearly demonstrate that TRAM-34 inhibited bronchial remodeling, eosinophil recruitment, and Th2 cytokine production in the airways. These findings raise the question of whether TRAM-34 is specific to BSM cells in our model. These effects probably occur through the involvement of several resident cells (BSM cells and fibroblasts) and inflammatory cells (T cells, lung mast cells, and macrophages), which play important roles in the pathophysiology of asthma. This ability of $K_{Ca}3.1$ blockade to target multiple cells in the asthmatic airway may present a distinct therapeutic advantage, because targeting a single cell type or mediator has often failed to provide significant and persistent clinical benefits.

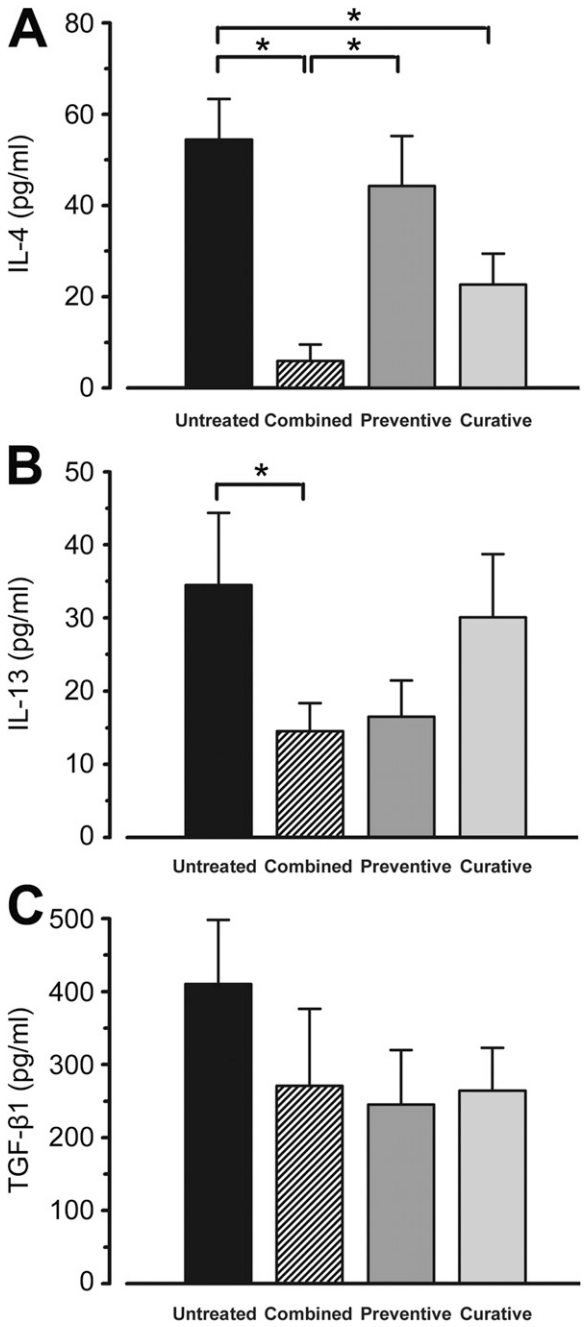

Figure 5. Effects of TRAM-34 on IL-4, IL-13, and TGF-β1 production in BAL fluid. OVA-sensitized/challenged mice received daily subcutaneous injections of TRAM-34 or its vehicle Miglyol-812 from Day −7 to Day 75. IL-4, IL-13, and TGF-β1 concentrations were measured using ELISA in BAL fluid obtained on Day 80. OVA mice received Miglyol-812 from Day −7 to Day 75 (untreated group, *solid bars*), or TRAM-34 from Day −7 to Day 75 (combined treatment, *hatched bars*), or TRAM-34 from Day −7 to Day 20 and Miglyol-812 from Days 21–75 (preventive treatment, *dark gray bars*), or Miglyol-812 from Day −7 to Day 20 and TRAM-34 from Day 21 to Day 75 (curative treatment, *light gray bars*) ($n = 8$ per group). Data represent the mean ± SEM. *$P < 0.05$ between populations within an experimental condition, using the Kruskal-Wallis test along with the multiple-comparison z-test.

Our study contains two important clinical implications that should be taken into consideration when designing clinical trials of $K_{Ca}3.1$ blockade in asthma. First, the ability of curative treatment with TRAM-34 to prevent and perhaps reverse the increased BSM mass suggests that $K_{Ca}3.1$ blockade has the potential to attenuate the decline in forced expiratory volume in 1 second (FEV_1). This occurs in many subjects with longstanding, often severe asthma (4), and appears not to be inhibited by corticosteroids (2). Second, airway eosinophilia plays an important role in the pathogenesis of severe asthma exacerbations (46). The ability of curative $K_{Ca}3.1$ blockade to attenuate airway eosinophilia suggests that $K_{Ca}3.1$ blockers might therefore reduce the frequency of severe asthma exacerbations, and might be particularly helpful in the group of patients with severe disease and relative corticosteroid resistance. Importantly, testing the effects of $K_{Ca}3.1$ blockade on fixed airflow obstruction, the decline in FEV_1, and eosinophilic exacerbations of asthma will require appropriately designed trials lasting many months.

In conclusion, $K_{Ca}3.1$ blockade has the potential to attenuate the development of fixed airflow obstruction in asthma and perhaps reverse it, and the potential to reduce the frequency of severe eosinophilic exacerbations of asthma. An orally bioavailable $K_{Ca}3.1$ blocker, senicapoc (ICA-17043), was well tolerated in Phase II and III trials for human sickle-cell disease (47, 48). Therefore the potential exists for the rapid translation of our current results to the clinic.

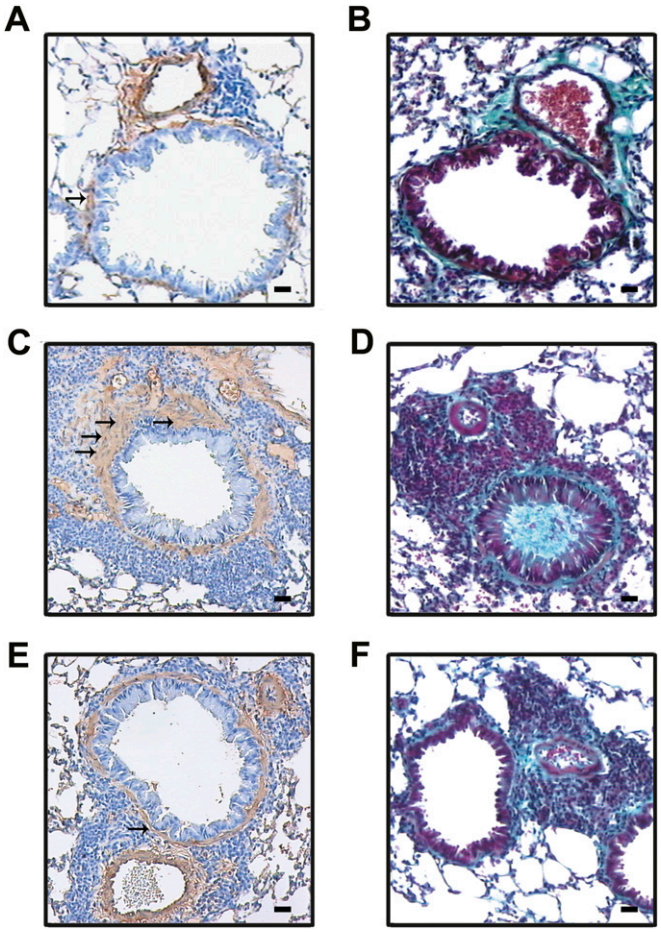

Figure 6. Representative optic microscopic images from lung sections obtained from control mice (*A* and *B*) and OVA-sensitized/challenged mice treated with either Miglyol-812 (*C* and *D*) or TRAM-34 (*E* and *F*) from Day −7 to Day 75. Lung slices were stained with either α–smooth muscle actin antibody (*A*, *C*, and *E*) or Masson trichrome (*B*, *D*, and *F*) on Day 80. Bronchial smooth muscle is visualized (*arrows*). *Scale bars* represent 50 μm (×100 magnification).

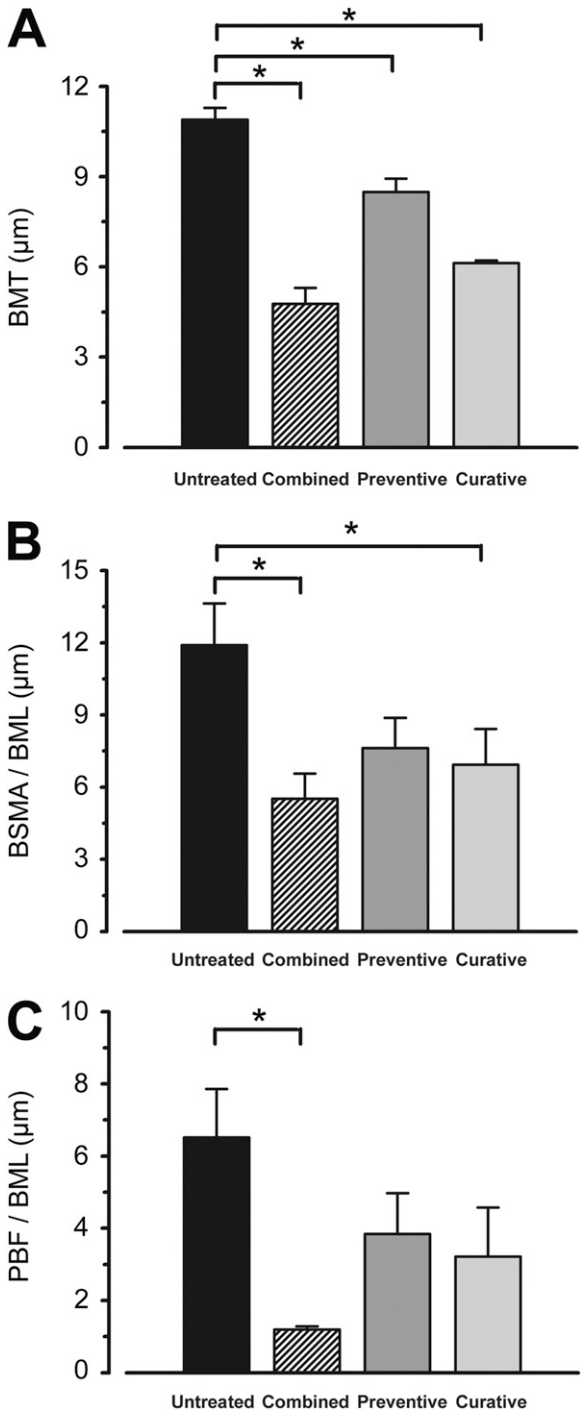

Figure 7. Effects of TRAM-34 on bronchial remodeling in a chronic model of murine asthma. OVA-sensitized/challenged mice received daily subcutaneous injections of TRAM-34 or its vehicle Miglyol-812 from Day −7 to Day 75. Histological analysis was performed on lung sections stained with α-smooth muscle actin (*A* and *B*) or Masson trichrome (*C*) on Day 80. OVA mice received Miglyol-812 from Day −7 to Day 75 (untreated group, *solid bars*), or TRAM-34 from Day −7 to Day 75 (combined treatment, *hatched bars*), or TRAM-34 from Day −7 to Day 20 and Miglyol-812 from Days 21–75 (preventive treatment, *dark gray bars*), or Miglyol-812 from Day −7 to Day 20 and TRAM-34 from Days 21–75 (curative treatment, *light gray bars*) ($n = 8$ per group). BMT, subbasement membrane thickness; BSMA/BML, bronchial smooth muscle area/basement membrane length ratio; PBF/BML, peribronchial fibrosis/basement membrane length ratio. Data represent the mean ± SEM. *$P < 0.05$ between populations within an experimental condition, using the Kruskal-Wallis test along with the multiple-comparisons z-test.

Author disclosures are available with the text of this article at www.atsjournals.org.

Acknowledgments: The authors thank Mrs. Béatrice Martinez, Mrs. Elise Maurat, and Mr. Vincent Pitard for their technical assistance. The authors also thank Béatrice Jaspard, Annabel Reynaud, and Myriam Petit-Roussel from the histological INSERM U1034 technical facility for their high-quality technical support.

References

1. Jeffery PK. Remodeling in asthma and chronic obstructive lung disease. *Am J Respir Crit Care Med* 2001;164:S28–S38.
2. Girodet PO, Ozier A, Bara I, Tunon de Lara JM, Marthan R, Berger P. Airway remodeling in asthma: new mechanisms and potential for pharmacological intervention. *Pharmacol Ther* 2011;130:325–337.
3. Bousquet J, Jeffery PK, Busse WW, Johnson M, Vignola AM. Asthma: from bronchoconstriction to airways inflammation and remodeling. *Am J Respir Crit Care Med* 2000;161:1720–1745.
4. Pepe C, Foley S, Shannon J, Lemiere C, Olivenstein R, Ernst P, Ludwig MS, Martin JG, Hamid Q. Differences in airway remodeling between subjects with severe and moderate asthma. *J Allergy Clin Immunol* 2005;116:544–549.
5. Kaminska M, Foley S, Maghni K, Storness-Bliss C, Coxson H, Ghezzo H, Lemiere C, Olivenstein R, Ernst P, Hamid Q, *et al*. Airway remodeling in subjects with severe asthma with or without chronic persistent airflow obstruction. *J Allergy Clin Immunol* 2009;124:45–51.
6. Roth M, Johnson PR, Borger P, Bihl MP, Rudiger JJ, King GG, Ge Q, Hostettler K, Burgess JK, Black JL, *et al*. Dysfunctional interaction of c/EBPalpha and the glucocorticoid receptor in asthmatic bronchial smooth-muscle cells. *N Engl J Med* 2004;351:560–574.
7. Bara I, Ozier A, Tunon de Lara JM, Marthan R, Berger P. Pathophysiology of bronchial smooth muscle remodelling in asthma. *Eur Respir J* 2010;36:1174–1184.
8. Brightling CE, Bradding P, Symon FA, Holgate ST, Wardlaw AJ, Pavord ID. Mast-cell infiltration of airway smooth muscle in asthma. *N Engl J Med* 2002;346:1699–1705.
9. Berger P, Girodet PO, Begueret H, Ousova O, Perng DW, Marthan R, Walls AF, Tunon de Lara JM. Tryptase-stimulated human airway smooth muscle cells induce cytokine synthesis and mast cell chemotaxis. *FASEB J* 2003;17:2139–2141.
10. Brightling CE, Ammit AJ, Kaur D, Black JL, Wardlaw AJ, Hughes JM, Bradding P. The CXCL10/CXCR3 axis mediates human lung mast cell migration to asthmatic airway smooth muscle. *Am J Respir Crit Care Med* 2005;171:1103–1108.
11. El-Shazly A, Berger P, Girodet PO, Ousova O, Fayon M, Vernejoux JM, Marthan R, Tunon-de-Lara JM. Fraktalkine produced by airway smooth muscle cells contributes to mast cell recruitment in asthma. *J Immunol* 2006;176:1860–1868.
12. Begueret H, Berger P, Vernejoux JM, Dubuisson L, Marthan R, Tunon-de-Lara JM. Inflammation of bronchial smooth muscle in allergic asthma. *Thorax* 2007;62:8–15.
13. Yang W, Kaur D, Okayama Y, Ito A, Wardlaw AJ, Brightling CE, Bradding P. Human lung mast cells adhere to human airway smooth muscle, in part, via tumor suppressor in lung cancer–1. *J Immunol* 2006;176:1238–1243.
14. Girodet PO, Ozier A, Trian T, Begueret H, Ousova O, Vernejoux JM, Chanez P, Marthan R, Berger P, Tunon de Lara JM. Mast cell adhesion to bronchial smooth muscle in asthma specifically depends on CD51 and CD44 variant 6. *Allergy* 2010;65:1004–1012.
15. Woodman L, Siddiqui S, Cruse G, Sutcliffe A, Saunders R, Kaur D, Bradding P, Brightling C. Mast cells promote airway smooth muscle cell differentiation via autocrine up-regulation of TGF-beta 1. *J Immunol* 2008;181:5001–5007.
16. Ramos-Barbon D, Fraga-Iriso R, Brienza NS, Montero-Martinez C, Verea-Hernando H, Olivenstein R, Lemiere C, Ernst P, Hamid QA, Martin JG. T cells localize with proliferating smooth muscle alpha–actin$^+$ cell compartments in asthma. *Am J Respir Crit Care Med* 2010;182:317–324.
17. Johnson PR, Roth M, Tamm M, Hughes M, Ge Q, King G, Burgess JK, Black JL. Airway smooth muscle cell proliferation is increased in asthma. *Am J Respir Crit Care Med* 2001;164:474–477.
18. Trian T, Benard G, Begueret H, Rossignol R, Girodet PO, Ghosh D, Ousova O, Vernejoux JM, Marthan R, Tunon-de-Lara JM, *et al*. Bronchial smooth muscle remodeling involves calcium-dependent enhanced mitochondrial biogenesis in asthma. *J Exp Med* 2007;204:3173–3181.

19. Mahn K, Hirst SJ, Ying S, Holt MR, Lavender P, Ojo OO, Siew L, Simcock DE, McVicker CG, Kanabar V, *et al*. Diminished sarco/endoplasmic reticulum Ca^{2+} ATPase (SERCA) expression contributes to airway remodelling in bronchial asthma. *Proc Natl Acad Sci USA* 2009;106:10775–10780.
20. McCann JD, Welsh MJ. Calcium-activated potassium channels in canine airway smooth muscle. *J Physiol* 1986;372:113–127.
21. Marthan R, Martin C, Amédée T, Mironneau J. Calcium channel currents in isolated smooth muscle cells from human bronchus. *J Appl Physiol* 1989;66:1706–1714.
22. Bradding P, Wulff H. The K^+ channels K(Ca)3.1 and K(V)1.3 as novel targets for asthma therapy. *Br J Pharmacol* 2009;157:1330–1339.
23. Devor DC, Singh AK, Lambert LC, DeLuca A, Frizzell RA, Bridges RJ. Bicarbonate and chloride secretion in CALU-3 human airway epithelial cells. *J Gen Physiol* 1999;113:743–760.
24. Grunnet M, Rasmussen HB, Hay-Schmidt A, Klaerke DA. The voltage-gated potassium channel subunit, KV1.3, is expressed in epithelia. *Biochim Biophys Acta* 2003;1616:85–94.
25. Pena TL, Rane SG. The fibroblast intermediate conductance K(Ca) channel, FIK, as a prototype for the cell growth regulatory function of the IK channel family. *J Membr Biol* 1999;172:249–257.
26. Mark Duffy S, Berger P, Cruse G, Yang W, Bolton SJ, Bradding P. The K^+ channel $IK_{Ca}1$ potentiates Ca^{2+} influx and degranulation in human lung mast cells. *J Allergy Clin Immunol* 2004;114:66–72.
27. Shepherd MC, Duffy SM, Harris T, Cruse G, Schuliga M, Brightling CE, Neylon CB, Bradding P, Stewart AG. $K_{Ca}3.1$ Ca^{2+} activated K^+ channels regulate human airway smooth muscle proliferation. *Am J Respir Cell Mol Biol* 2007;37:525–531.
28. Cruse G, Singh SR, Duffy SM, Doe C, Saunders R, Brightling CE, Bradding P. Functional $K_{Ca}3.1$ K^+ channels are required for human fibrocyte migration. *J Allergy Clin Immunol* 2011;128:1303–1309.
29. Shumilina E, Lam RS, Wolbing F, Matzner N, Zemtsova IM, Sobiesiak M, Mahmud H, Sausbier U, Biedermann T, Ruth P, *et al*. Blunted IgE-mediated activation of mast cells in mice lacking the Ca^{2+}-activated K^+ channel $K_{Ca}3.1$. *J Immunol* 2008;180:8040–8047.
30. Cruse G, Duffy SM, Brightling CE, Bradding P. Functional $K_{Ca}3.1$ K^+ channels are required for human lung mast cell migration. *Thorax* 2006;61:880–885.
31. Lederlin M, Ozier A, Montaudon M, Begueret H, Ousova O, Marthan R, Berger P, Laurent F. Airway remodeling in a mouse asthma model assessed by *in-vivo* respiratory-gated micro-computed tomography. *Eur Radiol* 2010;20:128–137.
32. Henderson WR Jr, Tang LO, Chu SJ, Tsao SM, Chiang GK, Jones F, Jonas M, Pae C, Wang H, Chi EY. A role for cysteinyl leukotrienes in airway remodeling in a mouse asthma model. *Am J Respir Crit Care Med* 2002;165:108–116.
33. Wulff H, Miller MJ, Hansel W, Grissmer S, Cahalan MD, Chandy KG. Design of a potent and selective inhibitor of the intermediate-conductance Ca^{2+}-activated K^+ channel, $IK_{Ca}1$: a potential immunosuppressant. *Proc Natl Acad Sci USA* 2000;97:8151–8156.
34. Toyama K, Wulff H, Chandy KG, Azam P, Raman G, Saito T, Fujiwara Y, Mattson DL, Das S, Melvin JE, *et al*. The intermediate-conductance calcium-activated potassium channel $K_{Ca}3.1$ contributes to atherogenesis in mice and humans. *J Clin Invest* 2008;118:3025–3037.
35. Lundblad LK, Irvin CG, Adler A, Bates JH. A reevaluation of the validity of unrestrained plethysmography in mice. *J Appl Physiol* 2002;93:1198–1207.
36. Adler A, Cieslewicz G, Irvin CG. Unrestrained plethysmography is an unreliable measure of airway responsiveness in BALB/c and C57BL/6 mice. *J Appl Physiol* 2004;97:286–292.
37. Mionnet C, Buatois V, Kanda A, Milcent V, Fleury S, Lair D, Langelot M, Lacoeuille Y, Hessel E, Coffman R, *et al*. CX3CR1 is required for airway inflammation by promoting T helper cell survival and maintenance in inflamed lung. *Nat Med* 2010;16:1305–1312.
38. Takeda K, Hamelmann E, Joetham A, Shultz LD, Larsen GL, Irvin CG, Gelfand EW. Development of eosinophilic airway inflammation and airway hyperresponsiveness in mast cell–deficient mice. *J Exp Med* 1997;186:449–454.
39. Johnson JR, Pacitto SR, Wong J, Archer EW, Eirefelt S, Miller-Larsson A, Jordana M. Combined budesonide/formoterol therapy in conjunction with allergen avoidance ameliorates house dust mite–induced airway remodeling and dysfunction. *Am J Physiol Lung Cell Mol Physiol* 2008;295:L780–L788.
40. Woodruff PG, Dolganov GM, Ferrando RE, Donnelly S, Hays SR, Solberg OD, Carter R, Wong HH, Cadbury PS, Fahy JV. Hyperplasia of smooth muscle in mild to moderate asthma without changes in cell size or gene expression. *Am J Respir Crit Care Med* 2004;169:1001–1006.
41. Siddiqui S, Mistry V, Doe C, Roach K, Morgan A, Wardlaw A, Pavord I, Bradding P, Brightling C. Airway hyperresponsiveness is dissociated from airway wall structural remodeling. *J Allergy Clin Immunol* 2008;122:335–341.
42. Berry M, Morgan A, Shaw DE, Parker D, Green R, Brightling C, Bradding P, Wardlaw AJ, Pavord ID. Pathological features and inhaled corticosteroid response of eosinophilic and non-eosinophilic asthma. *Thorax* 2007;62:1043–1049.
43. Flood-Page P, Menzies-Gow A, Phipps S, Ying S, Wangoo A, Ludwig MS, Barnes N, Robinson D, Kay AB. Anti–IL-5 treatment reduces deposition of ECM proteins in the bronchial subepithelial basement membrane of mild atopic asthmatics. *J Clin Invest* 2003;112:1029–1036.
44. Grgic I, Kiss E, Kaistha BP, Busch C, Kloss M, Sautter J, Muller A, Kaistha A, Schmidt C, Raman G, *et al*. Renal fibrosis is attenuated by targeted disruption of $K_{Ca}3.1$ potassium channels. *Proc Natl Acad Sci USA* 2009;106:14518–14523.
45. Chen YJ, Raman G, Bodendiek S, O'Donnell ME, Wulff H. The $K_{Ca}3.1$ blocker TRAM-34 reduces infarction and neurological deficit in a rat model of ischemia/reperfusion stroke. *J Cereb Blood Flow Metab* 2011;31:2363–2374.
46. Haldar P, Brightling CE, Hargadon B, Gupta S, Monteiro W, Sousa A, Marshall RP, Bradding P, Green RH, Wardlaw AJ, *et al*. Mepolizumab and exacerbations of refractory eosinophilic asthma. *N Engl J Med* 2009;360:973–984.
47. Ataga KI, Smith WR, De Castro LM, Swerdlow P, Saunthararajah Y, Castro O, Vichinsky E, Kutlar A, Orringer EP, Rigdon GC, *et al*. Efficacy and safety of the gardos channel blocker, senicapoc (ICA-17043), in patients with sickle cell anemia. *Blood* 2008;111:3991–3997.
48. Ataga KI, Reid M, Ballas SK, Yasin Z, Bigelow C, James LS, Smith WR, Galacteros F, Kutlar A, Hull JH, *et al*. Improvements in haemolysis and indicators of erythrocyte survival do not correlate with acute vaso-occlusive crises in patients with sickle cell disease: a Phase III randomized, placebo-controlled, double-blind study of the gardos channel blocker senicapoc (ICA-17043). *Br J Haematol* 2011;153:92–104.

Online Data Supplement

The $K_{Ca}3.1$ blocker TRAM-34 attenuates airway remodeling and eosinophilia in a mouse asthma model

Pierre-Olivier Girodet, MD, PhD, Annaig Ozier, MD, PhD, Gabrielle Carvalho, PhD, Olga Ilina, MD, Olga Ousova, PhD, Alain-Pierre Gadeau, PhD, Hugues Begueret, MD, PhD, Heike Wulff, PhD, Roger Marthan, MD, PhD, Peter Bradding, DM and Patrick Berger, MD, PhD

Supplemental material and methods

Animals

Female BALB/c mice (5 weeks old, Elevage Janvier, Le Genest Saint Isle, France) were acclimatized for a week prior to starting the experiments. The Institutional Animal Ethics Committee approved all animal use procedures.

Chronic model of murine asthma

Mice were sensitized with i.p. injection of 100 µg ovalbumin (OVA, Sigma-Aldrich, Saint-Quentin-Fallavier, France) in 200 µl sterile NaCl 0.9% (B. Braun Medical, Boulogne Billancourt, France) without aluminium hydroxide, at Days 0 and 14 as described previously (E1). Mice were anesthetized with ketamine/xylazine (i.p., 50/5 µg/g mouse, Panpharma, Fougeres, France/Sigma-Aldrich) at Days 14, 27, 28, 29, 47, 61, 73, 74 and 75, and then challenged with 500 µg OVA in 30 µl NaCl 0.9% by nasal administration (E1, E2). The

control group received NaCl 0.9% i.p. at Days 0 and 14 and intranasally at Days 14, 27, 28, 29, 47, 61, 73, 74 and 75.

Study design

TRAM-34 (5-[(2-chlorophenyl)(diphenyl)methyl]-1*H*-pyrazole) was synthesized by H. Wulff as described previously (E3). It was dissolved in neutral oil (Miglyol-812, Caesar & Loretz GmbH, Hilden, Germany) and administered once daily subcutaneously at a dose of 120 mg/kg/day. Four groups of OVA-sensitized and challenged mice (OVA-mice) received daily injections of either (i) Miglyol from Days -7 to 75 (untreated group); (ii) TRAM-34 from Days -7 to 75 (i.e. prior to i.p. sensitization and during nasal challenge) (combined treatment group); (iii) TRAM-34 prior and during i.p. sensitization (Days -7 to 20) and Miglyol during nasal challenge (Days 21 to 75) (preventive treatment group); or (iv) Miglyol prior and during i.p. sensitization (Days -7 to 20) and TRAM-34 during nasal challenge (Days 21 to 75) (curative treatment group).

Determination of bronchial hyperresponsiveness

Non-specific BHR to methacholine (Sigma-Aldrich) was measured in both unrestrained conscious mice by single-chamber plethysmography and in anesthetized mice by invasive plethysmography (both from Emka Technologies, Paris, France). Both enhanced pause (Penh) parameter and lung resistance (Rs) were measured and averaged for 3 min, 30 sec after inhalation of normal saline or 8 mg/ml nebulized methacholine (E4, E5). Penh measurements were performed at Days 0, 20, and 76 and expressed as a ratio of Penh measured in response to methacholine to that with normal saline. Specific BHR to OVA was measured 4h after intranasal OVA challenge at Days 28 and 74. Lung Rs measurements were performed at Day 80 only.

Tissue sampling

Blood was recovered on Day 78 with a capillary tube from the retro-orbital plexus. Bronchoalveolar lavage (BAL) was obtained at Day 80 by cannulating the trachea with a 24-gauge catheter. The right lung was lavaged twice (each aliquot 0.3 ml; NaCl 0.9%). Total cell number was counted with a hemocytometer. Cytocentrifuge preparations (Cytospin 4, ThermoFisher Scientific, Courtaboeuf, France) were stained with Diff-Quik® (VWR International, Strasbourg, France). Differential cell counting was performed using standard morphological criteria in which 200 cells were counted per slide.

Anaesthetized mice were exsanguinated by cardiac puncture at Day 80 after the BAL. Bone marrow was washed out of the right femur and the tibia. The number of bone marrow cells was counted with a hemocytometer. The right and left lung tissues were dissected out. The right lungs were cut in 1 mm^3 fragments and digested in 2 mg/ml collagenase IA and 1 mg/ml DNase I (both from Sigma-Aldrich) for 30 min at 37°C. Lung cells were purified with a 70-µm cell strainer (BD Biosciences – Pharmingen, Le Pont de Claix, France) (E6). Left lungs and liver were fixed in formaldehyde and embedded in paraffin.

Histological and immunohistochemical analysis

Histological analysis was performed on 4 µm-thick lung slices stained with haematoxylin-eosin-safran or Masson's trichrome. Immunohistochemistry of lung specimens was processed as previously described (E1). Briefly, sections were incubated with an anti-mouse α-smooth muscle actin (αSMA) or the irrelevant control Ab (both from Sigma-Aldrich), followed by biotinylated rabbit secondary Ab (Dako) and the streptavidin-biotin horseradish-peroxidase complex (Dako). After rinsing in phosphate buffered saline, 1 mg/ml 3,3'-diaminobenzidine tetrahydrochloride (Dako) in the presence of 0.02% H_2O_2 was used as a substrate to develop a

peroxide-dependent brown color reaction. Finally, the sections were rinsed and counterstained with Mayer's haematoxylin. BSM was identified by a pathologist in a blinded fashion using both morphological characteristics and αSMA staining as described previously (E7). Various quantitative parameters were assessed using Quancoul® (Quant'Image, Bordeaux, France) software at magnifications of x100 to x400 (E8). The wall area (defined by the sum of epithelial, submucosal and BSM areas) and the BSM area were automatically delineated from a mean of 5 bronchi per mouse. We manually delineated the sub-basement membrane thickness (BMT) using Quancoul® software at magnifications of x400. We averaged 5 distinct measurements per bronchus. We paid special attention to select 5 non-cartilaginous bronchi grossly perpendicular to the slice (big axis/small axis less than 1.3), per mouse. Indeed, non-perpendicular bronchi could have induced error measurements due to partial volume effects. The peribronchial fibrosis (PBF) was also manually delineated. The number of nucleated cells was automatically counted within the peribronchial space as described previously (E1).

In another set of experiments, lungs were immediately fixed after harvesting in buffered formalin for overnight. Endothelial cells were identified with rat anti-mouse CD31 antibody (clone ER-MP12, BMA Biomedicals, Augst, Switzerland). Primary antibodies were sequentially stained with biotin-conjugated secondary antibodies (GE Healthcare Europe GmbH, Velizy-Villacoublay, France) and streptavidin-HRP complex. Then, the stain was developed with a DAB substrate and tissues were counterstained with hematoxylin using the automated Benchmark XT platform (Ventana Medical Systems, Tucson, AZ, USA) and according to the manufacturer's recommendations.

Flow cytometry

Cells isolated from blood and lung digests were incubated with anti-CD16/CD32 Ab (BD Biosciences) to block FcγRIII/II receptors before staining with a specific Ab. The following

Abs were used for surface staining: FITC-conjugated anti-CD3-ε, PE-conjugated anti-CD4, PE-Cy5 anti-CD8a, PE-conjugated anti-CD90.2, FITC-conjugated anti-CD117 (*c-kit*), PE-conjugated anti-CD49b/Pan-NK cells (all from BD Biosciences - Pharmingen), PE-Cy5-conjugated anti-CD25 (eBioscience, Paris, France) and respective isotype control Abs. For intracellular staining of Foxp3 (E9), cells were fixed and permeabilized with Foxp3 staining buffer (eBioscience), then stained with FITC conjugated anti-Foxp3 mAb (eBioscience). After two additional washes, cells were analyzed for their fluorescence intensity using flow cytometry (FACSCanto™ Flow Cytometer and FACSDiva™ software, BD Biosciences).

Statistical analysis

Values are expressed as the mean ± SEM. Statistical analysis was performed using NCSS 2001® software. Data were analyzed by Mann & Whitney test. Multiple comparisons were performed by means of Kruskall-Wallis analysis of variance, with the use of multiple comparison z tests. A P value < 0.05 was considered statistically significant.

References

E1. Lederlin M, Ozier A, Montaudon M, Begueret H, Ousova O, Marthan R, Berger P, Laurent F. Airway remodeling in a mouse asthma model assessed by in-vivo respiratory-gated micro-computed tomography. *Eur Radiol* 2010;20:128-137.

E2. Henderson WR, Jr., Tang LO, Chu SJ, Tsao SM, Chiang GK, Jones F, Jonas M, Pae C, Wang H, Chi EY. A role for cysteinyl leukotrienes in airway remodeling in a mouse asthma model. *Am J Respir Crit Care Med* 2002;165:108-116.

E3. Wulff H, Miller MJ, Hansel W, Grissmer S, Cahalan MD, Chandy KG. Design of a potent and selective inhibitor of the intermediate-conductance Ca2+-activated K+ channel, IKCa1: A potential immunosuppressant. *Proc Natl Acad Sci U S A* 2000;97:8151-8156.

E4. Dohi M, Tsukamoto S, Nagahori T, Shinagawa K, Saitoh K, Tanaka Y, Kobayashi S, Tanaka R, To Y, Yamamoto K. Noninvasive system for evaluating the allergen-specific airway response in a murine model of asthma. *Lab Invest* 1999;79:1559-1571.

E5. Adler A, Cieslewicz G, Irvin CG. Unrestrained plethysmography is an unreliable measure of airway responsiveness in BALB/c and C57BL/6 mice. *J Appl Physiol* 2004;97:286-292.

E6. Doherty TA, Soroosh P, Khorram N, Fukuyama S, Rosenthal P, Cho JY, Norris PS, Choi H, Scheu S, Pfeffer K, et al. The tumor necrosis factor family member light is a target for asthmatic airway remodeling. *Nat Med* 2011;17:596-603.

E7. Berger P, Girodet PO, Begueret H, Ousova O, Perng DW, Marthan R, Walls AF, Tunon de Lara JM. Tryptase-stimulated human airway smooth muscle cells induce cytokine synthesis and mast cell chemotaxis. *FASEB J* 2003;17:2139-2141.

E8. Berger P, Lavallee J, Rouiller R, Laurent F, Marthan R, Tunon-de-Lara JM. Assessment of bronchial inflammation using an automated cell recognition system based on colour analysis. *Eur Respir J* 1999;14:1394-1402.

E9. D'Alessio FR, Tsushima K, Aggarwal NR, West EE, Willett MH, Britos MF, Pipeling MR, Brower RG, Tuder RM, McDyer JF, et al. CD4+CD25+Foxp3+ Tregs resolve experimental lung injury in mice and are present in humans with acute lung injury. *J Clin Invest* 2009;119:2898-2913.

Supplementary figures legends

Figure E1

Chronic airway exposure of mice to OVA induced accumulation of eosinophils and lymphocytes in the lung. BAL fluid was obtained at Day 20 (A, C, E) or at Day 80 (B, D, F) in another set of experiments. BALB/c mice received either OVA (black bars, n=11) or normal saline (white bars, n=11). Data are the mean ± the SEM. *, $P < 0.05$ using Mann & Whitney test.

Figure E2

Chronic airway exposure of mice to OVA induced inflammatory cell recruitment within the lung. BALB/c mice received either OVA (black bars, n=7) or normal saline (white bars, n=7). The total number of lung cells (A), the absolute number of CD4 T cells (B) and CD4/CD8 ratio (C) were assessed at Day 80 using flow cytometry. Data are the mean ± the SEM. *, $P < 0.05$ using Mann & Whitney test.

Figure E3

Representative optic microscopic images from lung sections obtained from control mice (A) and OVA-sensitized/challenged mice (B). Lung slices were stained with anti-CD31 antibody at Day 80. Scale bars represent 50 µm (200x magnification).

Figure E4

Representative optic microscopic images from liver sections obtained from OVA-sensitized/challenged mice treated by either Miglyol from Day -7 to Day 75 (untreated group, A), or TRAM-34 from Day -7 to Day 75 (combined treatment, B), or TRAM-34 from Day-7

to Day 20 and Miglyol from Day 21 to Day 75 (preventive treatment, C), or Miglyol from Day -7 to Day 20 and TRAM-34 from Day 21 to Day 75 (curative treatment, D). BALB/c mice received normal saline only in another set of experiment (E). Liver slices were stained with haematoxylin-eosin-safran at Day 80. Scale bars represent 50 µm (200x magnification).

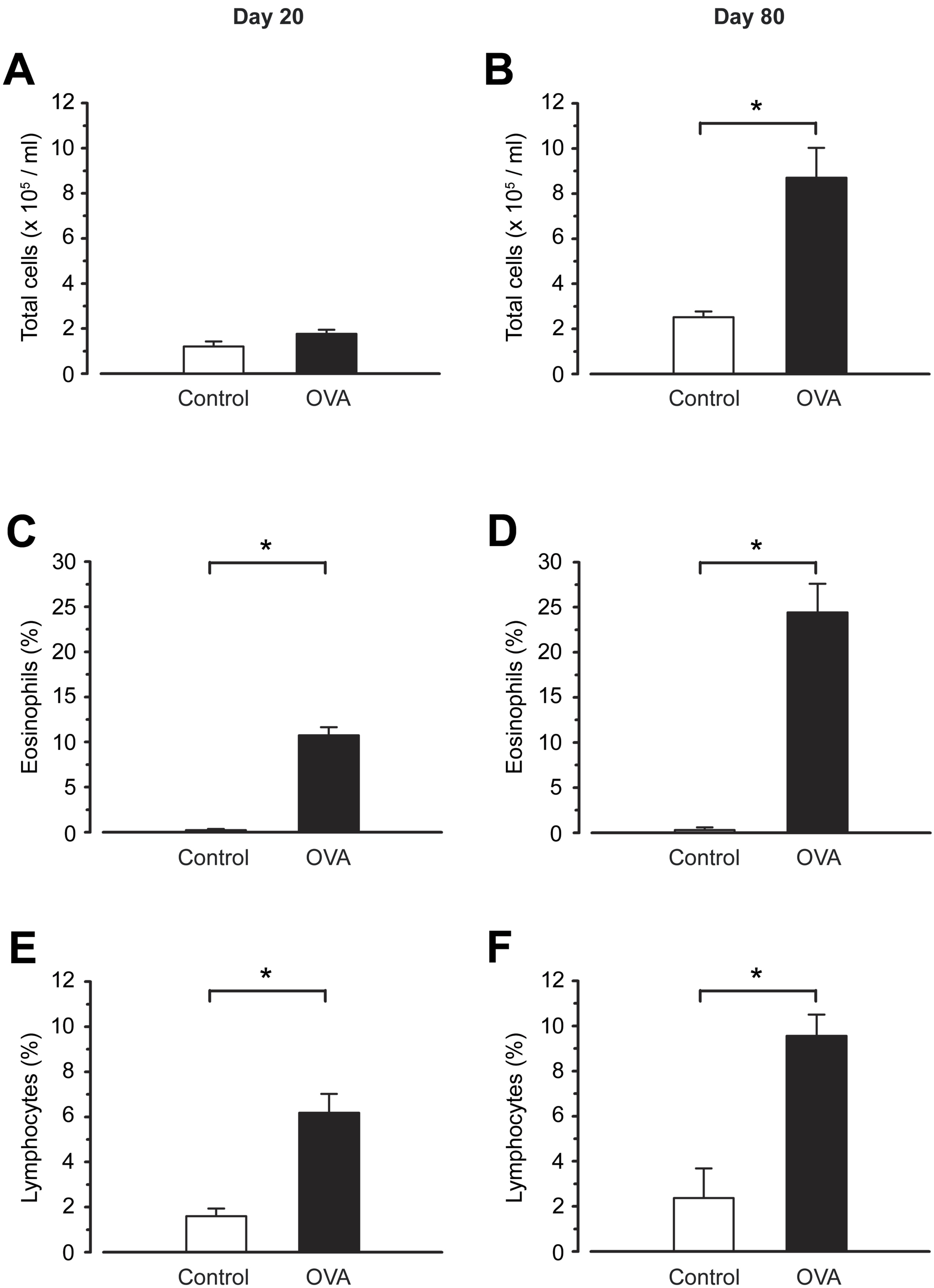
Day 20
Day 80
A
B
C
D
E
F
Total cells (x 10^5 / ml)
Eosinophils (%)
Lymphocytes (%)
Control
OVA
*

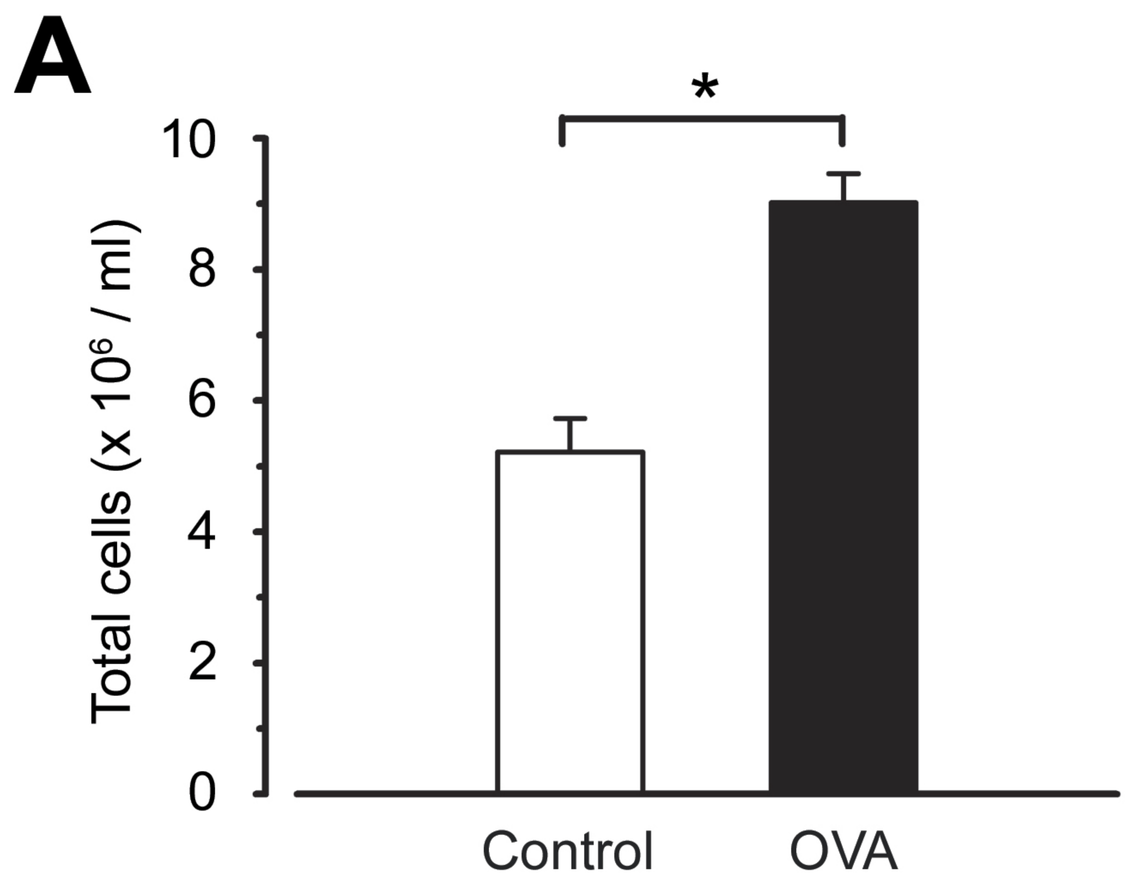
A
*
Total cells (x 10^6 / ml)
10
8
6
4
2
0
Control
OVA

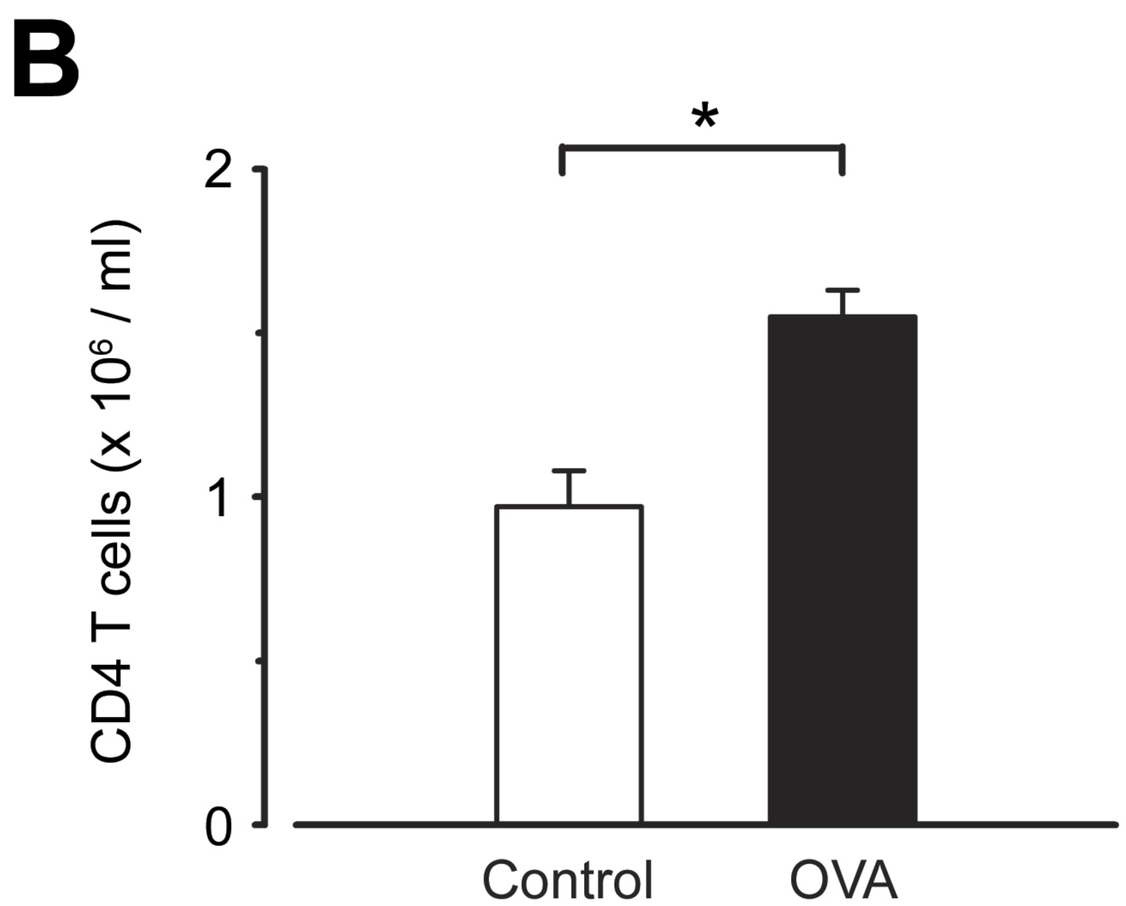
B
*
CD4 T cells (x 10^6 / ml)
2
1
0
Control
OVA

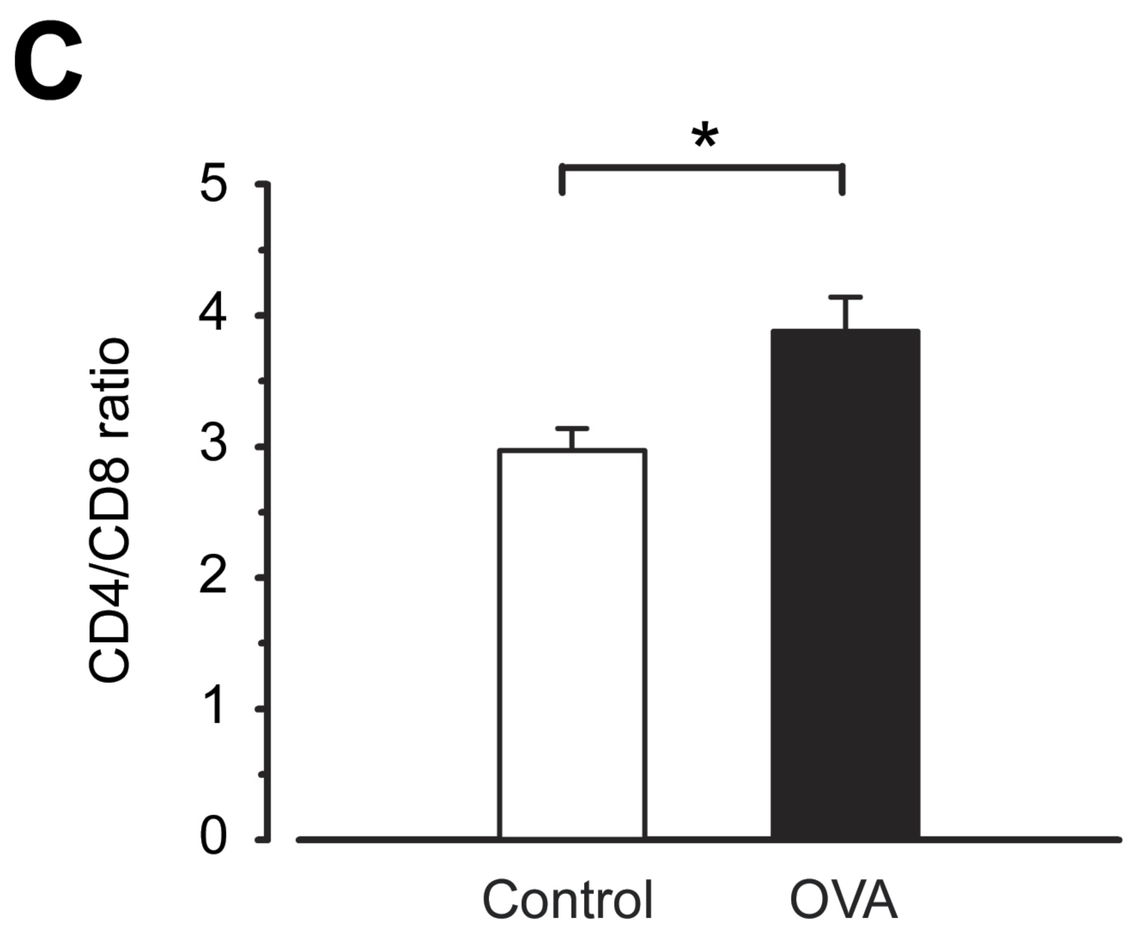
C
*
CD4/CD8 ratio
5
4
3
2
1
0
Control
OVA

A

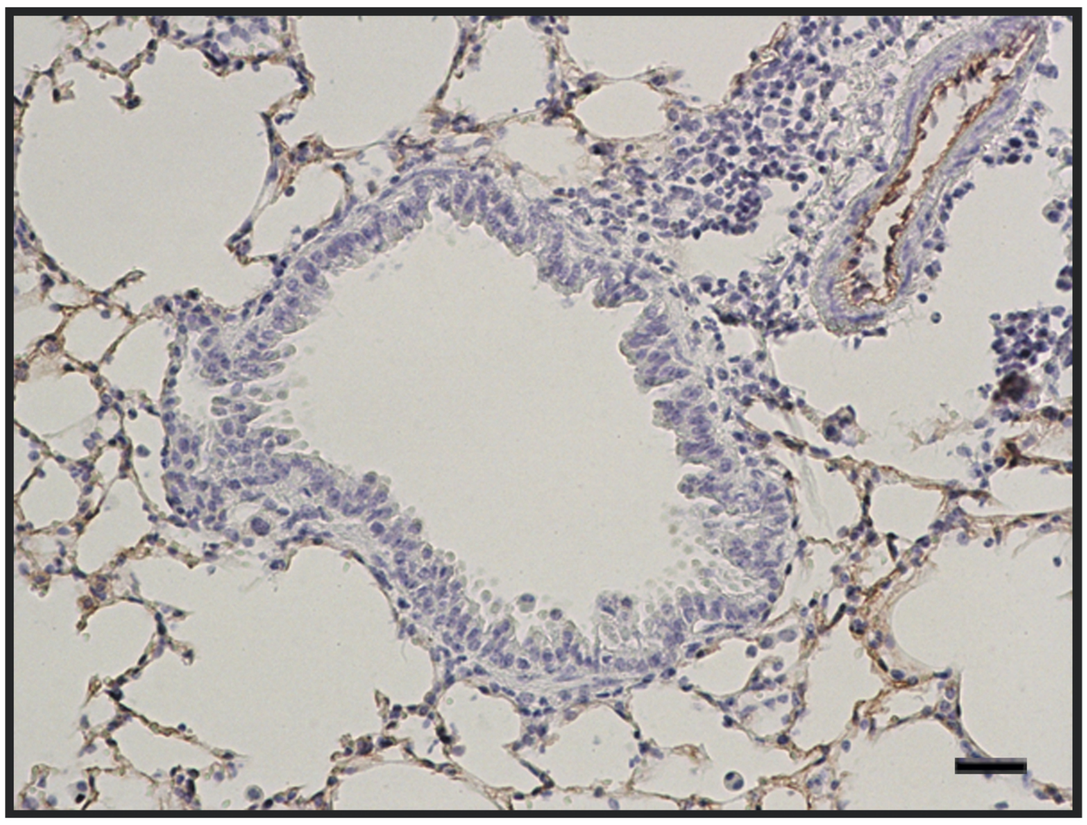

B

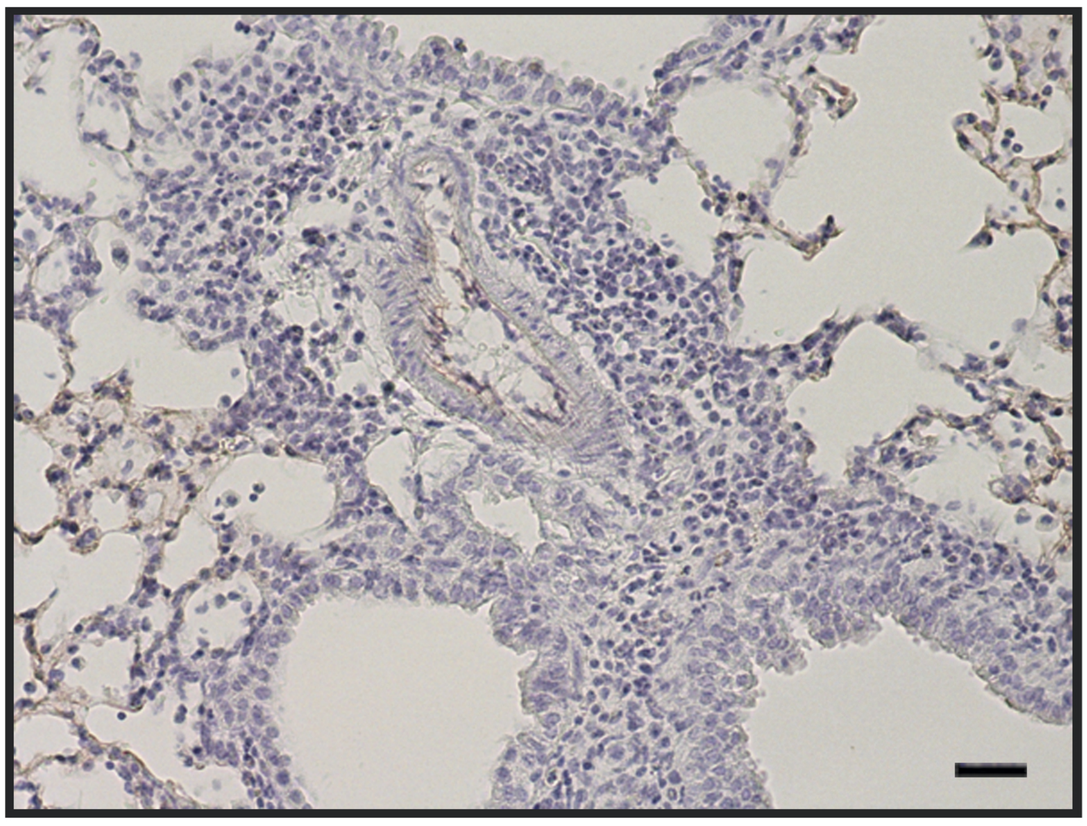

A

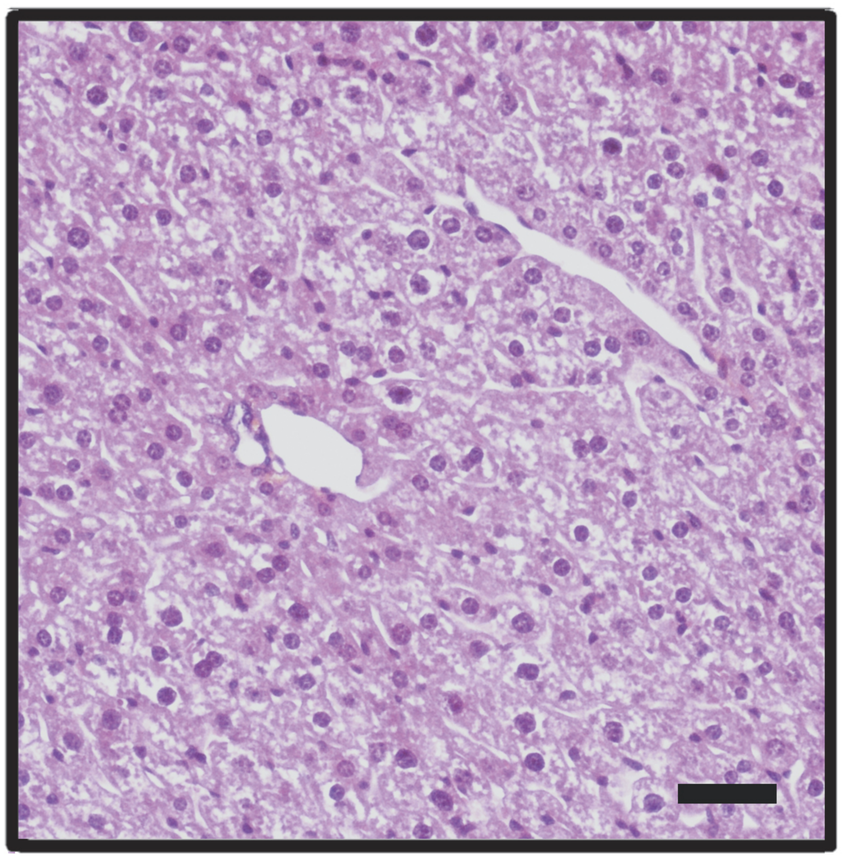

B

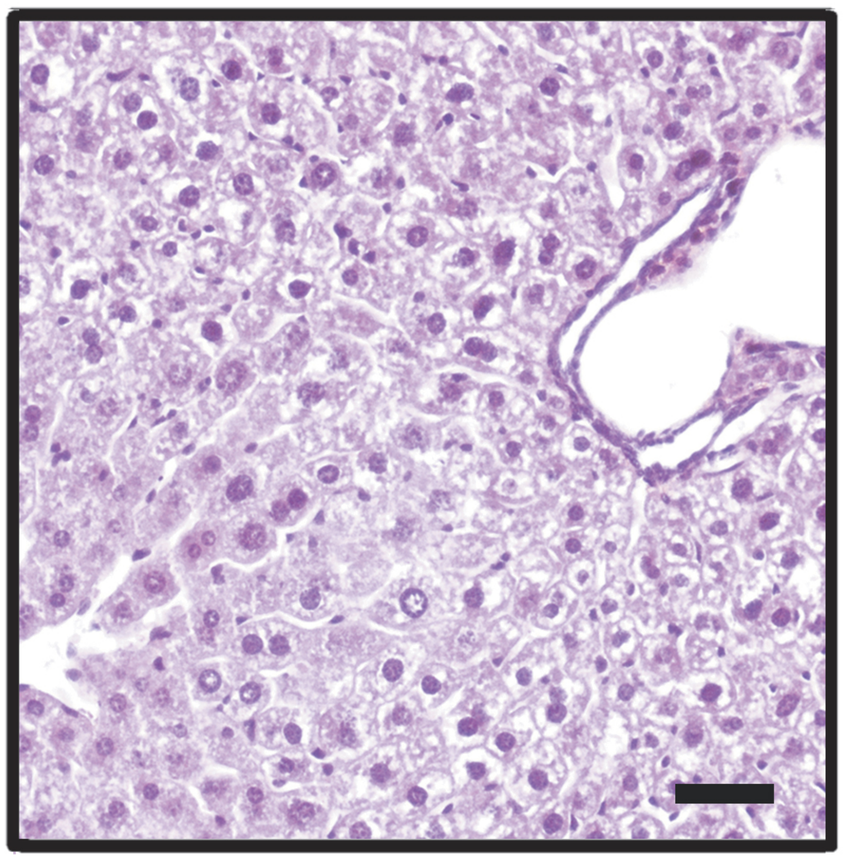

C

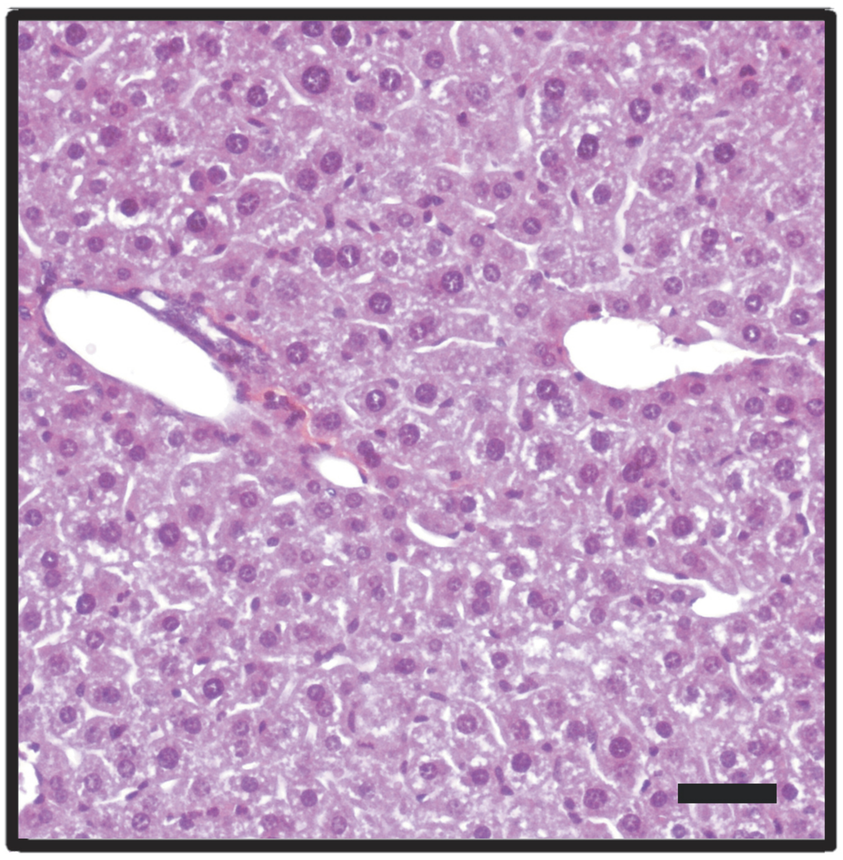

D

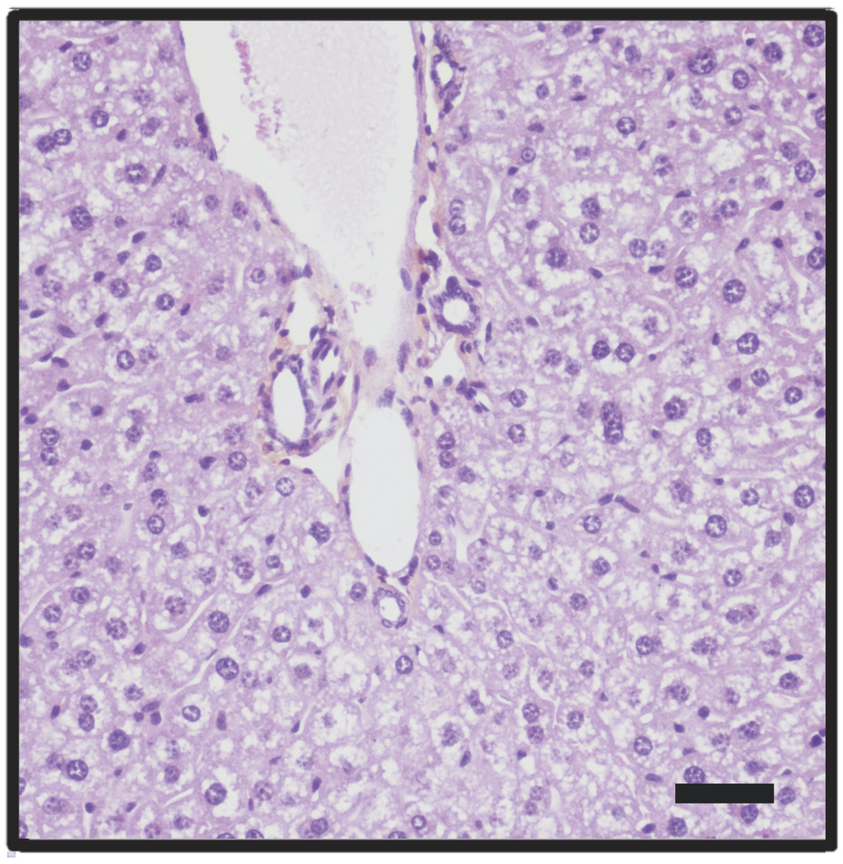
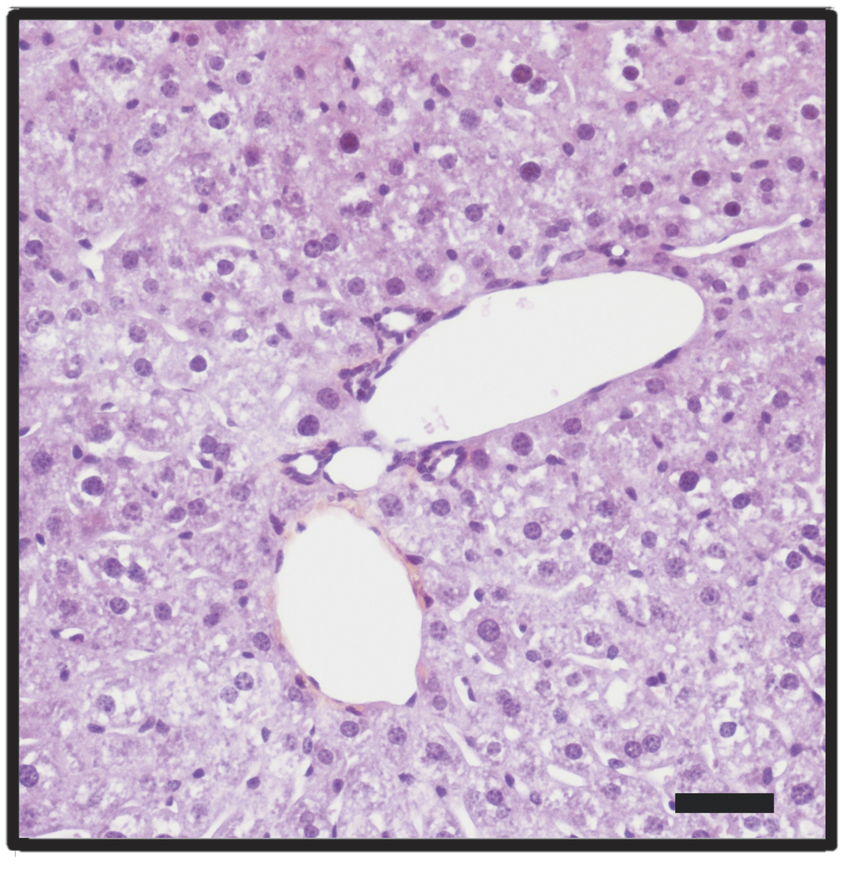
E